FIBER-OPTIC SENSORS FOR REAL-TIME TEMPERATURE MONITORING IN MINIMALLY INVASIVE THERMO-THERAPIES

Sultan Sovetov, BEng in Electrical and Electronic Engineering

Submitted in fulfilment of the requirements for the degree of Master of Science in Electrical and Electronic Engineering

School of Engineering

Department of Electrical and Electronic Engineering

Nazarbayev University

53 Kabanbay Batyr Avenue, Astana, Kazakhstan, 010000

Supervisors: Daniele Tosi, Ikechi A. Ukaegbu

January 2019

DECLARATION

I hereby, declare that this manuscript, entitled "*Fiber-Optic Sensors for Real-Time Temperature Monitoring",* is the result of my own work except for quotations and citations which have been duly acknowledged.
I also declare that, to the best of my knowledge and belief, it has not been previously or concurrently submitted, in whole or in part, for any other degree or diploma at Nazarbayev University or any other national or international institution.

Name: Sultan Sovetov
Date: 12.12.2018

Abstract

There are various procedures for the tumor removal process, which include surgical procedures and thermal ablation processes. The surgical method is considered as the traditional one; however, the thermal ablation processes are conducted as well. These thermal ablation processes require temperature change monitoring of the area of the tissue, where the heat is applied. In this work, it is suggested to use fiber-optic sensors for temperature change monitoring in minimally invasive thermo-therapies for cancer care. The comparison of fiber-optic sensors, based on the 5-element FBG array, the CFBG, and the OBR, all of which are operating in real-time and suggested to be used for the temperature change monitoring in minimally invasive thermo-therapies for cancer care was provided in this work. The following criteria was used to compare these temperature sensing technologies: spatial resolution, temperature sensing range, hardware setup, time required for temperature change reconstruction and cost. There were experiments conducted in both the laboratory and in the clinical settings. Also, various recommendations and improvements for future experiments were provided as well. Considering the minimal invasiveness, low-cost and operation in real-time, all of the previously mentioned fiber-optic sensors could be used for the given application; however, the CFBG sensor is suggested to be the most suitable one compared to its alternatives, which are the 5-element FBG array and the OBR-based sensors.

Acknowledgments

I would like to thank my supervisors, Dr. Daniele Tosi and Dr. Ikechi A. Ukaegbu, for guiding and supporting me in the preparation of this work. I am also grateful for an opportunity to deepen my knowledge in the field of optical communication, fiber-optic sensors and their application in minimally invasive thermo-therapies.

Table of Contents

List of Abbreviations and Symbols

FBG	Fiber Bragg grating
CFBG	Chirped fiber Bragg grating
DTS	Distributed temperature sensor
TC	Thermocouple
TA	Thermal ablation
RFA	Radiofrequency ablation
HIFU	High intensity focused ultrasound
LA	Laser ablation
MWA	Microwave ablation
MRI	Magnetic resonance imaging

List of Tables and Figures

List of Publications

Korganbayev, S, Orazayev, Y, Sovetov, S, et al., 'Detection of thermal gradients through fiber-optic Chirped Fiber Bragg Grating (CFBG): Medical thermal ablation scenario' *Optical Fiber Technology*, vol 41, pp. 48-55, 2018. (Invited paper).

Korganbayev, S, Orazayev, Y, Sovetov, S, et al., 'Thermal Gradient Estimation with Fiber-Optic Chirped FBG Sensors: Experiments in Biomedical Applications' *IEEE Sensors Conference*, Glasgow, United Kingdom, 10/30/17 - 11/1/17, 2017.

Chapter 1 – Introduction

The objective of this work was to conduct a comparative study for various fiber-optic sensing technologies, which are, in this work, are used for temperature change monitoring in minimally invasive thermo-therapies for cancer care and to make sure that these technologies operate in real-time. There are 3 fiber-optic sensing technologies compared in this work, which are based on fiber Bragg grating (FBG), chirped fiber Bragg grating (CFBG) and standard fiber connected to an optical backscatter meter. The main criteria used to compare these technologies are spatial resolution, temperature sensing range, hardware setup, time required for temperature reconstruction, and cost. For the sensing technologies based on FBG and CFBG, a system was built, called an interrogator. This system involved such components as a light source [17], a spectrometer [18], a coupler and a fiber-optic sensor, which , in this work, is either an FBG or a CFBG sensor. The temperature sensing technology based on a standard fiber connected to an optical backscatter meter is also considered in this work and compared to an FBG array and a CFBG sensors. In this work, the necessary experimental data is gathered by conducting thermal ablation experiments, which are either radiofrequency ablation (RFA) or high intensity focused ultrasound ablation (HIFU). There are various applications of the fiber-optic temperature sensing technologies, which include medical applications. In this work, considering minimal invasiveness and thin structure of the sensors, it is suggested to use these temperature sensing technologies for temperature change monitoring in minimally invasive thermo-

therapies for cancer care. The work is organized in the following way. Initially, the theoretical background is presented for the temperature sensing technologies used in this work, starting with a 5-element FBG array sensor, as it is the simplest one and gives the necessary foundation for explaining the working principle of a CFBG sensor, which is described next, and, finally, the working principle of an optical backscatter meter is explained. In addition to the fiber-optic temperature sensing technologies, the thermal ablation technologies are presented, including radiofrequency ablation (RFA), high intensity focused ultrasound (HIFU) ablation, laser ablation (LA), and microwave ablation (MWA). The alternative technologies and techniques are described in this section as well. The next chapter describes the conducted work, which involved conducting thermal ablation (TA) experiments both in the laboratory and in the clinical settings, primarily focusing on the results from the RFA and the HIFU ablation experiments, which were used as a mean for comparing the fiber-optic temperature sensing technologies and their combination with various thermal ablation techniques. The following chapter is used to present the results and the necessary analysis of the results. In addition, the possible improvements of the system used in the project and the recommendations for conducting future experiments are added as well. This section also states that based on the given criteria of spatial resolution, temperature sensing range, hardware setup, time required for temperature reconstruction, and cost, it is suggested that the CFBG sensors are the most suitable ones for the given application of these sensors in minimally invasive thermo-therapies for cancer care.

Chapter 2 – Literature and Technology Review

This section provides the necessary theoretical background for the technologies, which were used in this work, as well as their alternatives. Some of the technologies described in this section have been used by researchers for a long time, while other technologies are considered relatively new, especially, taking into account the application of these technologies for temperature change monitoring in minimally invasive thermo-therapies. This section is split into 2 parts and is organized as follows. Initially, the fiber-optic temperature sensing technologies, which were used in this work, are described. Secondly, the thermal ablation (TA) techniques used in this work are presented. There are also alternative approaches for conducting thermal ablation (TA) processes that are mentioned and the technique that doctors currently use instead of temperature change monitoring in a tumor removal process is described as well.

2.1 Fiber-Optic Sensors

As it was previously mentioned, in this work. 3 fiber-optic temperature change monitoring technologies are compared, which are a 5-element FBG array sensor, a CFBG sensor and a standard fiber connected to an optical backscatter meter. All of these sensors can be used for distributed temperature change monitoring and are, therefore, described in this section. An example of a typical fiber optic sensor is shown

in Figure 2.1.1. As can be seen, one of the most important physical characteristics of a typical fiber optic sensors is its thinness, which allows it to be used in minimally invasive medical operations. The fiber-optic sensors are also immune from the electromagnetic interference [24, 25]. The sensing region of a 5-element FBG array and a CFBG sensors are limited to a certain portion of the total length of the optical cable, shown in Figure 2.1.1, [23]. Typically, the sensing region of a 5-elements FBG array sensor is 0.05 m, while for a CFBG sensor, it is either 0.015 or 0.05 m. However, using an optical backscatter meter allows monitoring the changes in temperature along the whole length of the fiber optic sensor, which, in this work, is a standard fiber. This is an advantage of the optical backscatter meter.

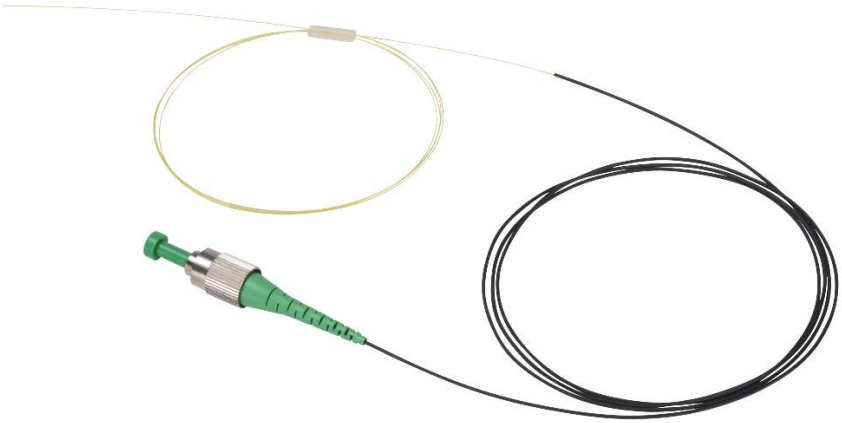

Figure 2.1.1: A visual representation of a typical fiber optic sensor

In this paragraph, the working principle of an FBG array sensor is explained. FBG array sensors are among the most popular fiber-optic sensors [4]. There are various FBG array sensors with different characteristics. In this work, it was decided to use an FBG array, which was comprised of 5 FBGs placed at a distance of 0.01 m

from each other. The total length of this sensor was 0.05 m. As a result, this sensor could measure changes in temperature at 5 points along the sensor over the distance of 0.05 m [4], [16], [26]. Therefore, this sensor can be used as a distributed temperature sensor (DTS). Prior to describing the working principle of an FBG array, it is useful to explain how a single FBG operates. Initially, it is required to build a setup, which consists of a light source, a spectrometer, a coupler, a fiber-optic sensor and a computer [16], [23]. The light source is a vital part of the system, as it is used to pass the light through the optical cables and, eventually, reaches the FBG array [26]. The wavelengths satisfying the Bragg condition are then reflected and reach the spectrometer via the optical cables. This spectrometer is used to evaluate the reflected light, and the data is then displayed on a computer. Therefore, the first step is to connect all these components and turn on the power supply. Once the power supply is turned on, the light will start passing through the optical fiber and will reach a single FBG connected at the end of the optical fiber. Considering that a single FBG is connected, a narrow spectrum is reflected having a peak value at a certain wavelength, as shown in Figure 2.1.2 [3].

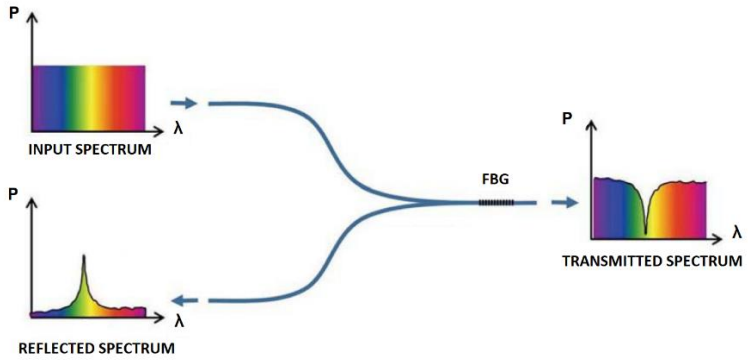

Figure 2.1.2: The working principle of a single FBG

This wavelength is called the Bragg wavelength and serves as the base for temperature reconstruction [3], [26]. Once the temperature is increased, this spectrum will move to the right. If the temperature is decreased, the whole spectrum will move to the left. The spectrometer is used to track the variations in this spectrum, which is then analyzed using a software on a computer. This software is called I-MON 512 USB Evaluation Software, which allows observing the changes in the spectrum. Another I-MON software is used to record these spectrum variations and saves them as a text file. The data in this text file is used to reconstruct the temperature profile based on the changes in the spectrum using a code written in MATLAB. Combining 5 of these single FBGs will make an FBG array, which is capable of monitoring the changes in temperature at 5 points placed at 0.01 m from each other over a distance of 0.05 m. An example of a spectrum of an FBG array, which is subject to changes in temperature, is shown in Figure 2.1.3.

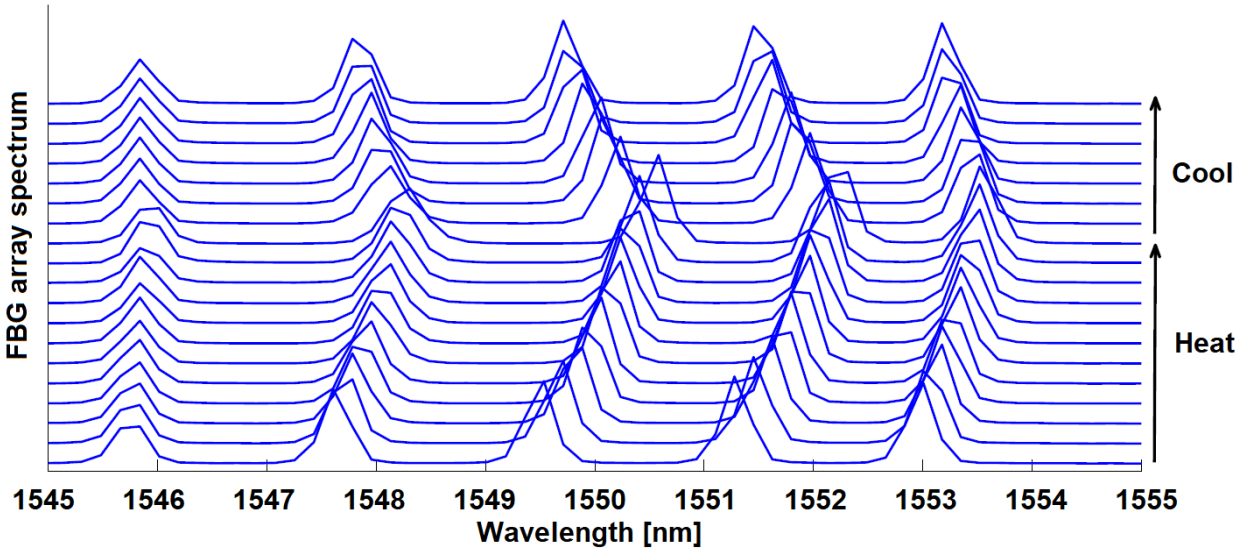

Figure 2.1.3: The changes in spectrum of an FBG array according to the variations in applied temperature

As can be seen from Figure 2.1.3, there are 5 peaks that correspond to 5 points at which the changes in temperature are observed. It can be seen that when the spectrum moves to the right, the temperature applied at the sensor is increased, and the peak wavelengths that moves the most is where the highest temperature was applied. It can be seen that the first peak of the FBG array experiences minimal changes, while the third peak wavelengths moves significantly. This indicates that the highest temperature was applied at the center of the FBG array sensor. Once the changes in spectrum have been recorded and saved in a text file, the temperature reconstruction process for an FBG array is started. To accomplish this task, it is required to review several equations. First of all, it is necessary to define the reference Bragg wavelength [2], [4].

$$\lambda_{B,0} = 2n_{eff}\Lambda \tag{2.1.1}$$

where N is the subscript that denotes the N-th grating, n_{eff} is the effective refractive index and Λ is the grating period, which is the length between the gratings.

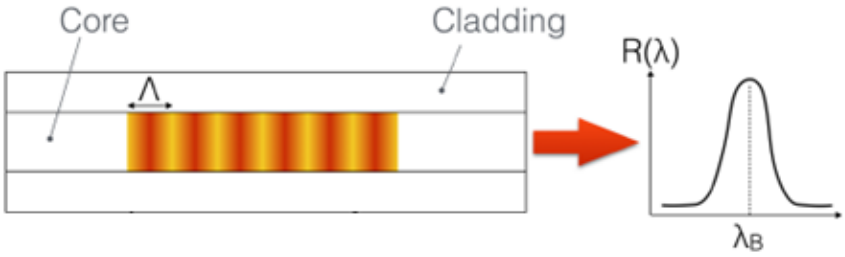

Figure 2.1.4: A representation of the grating period for a single FBG

The next step is to review the dependency of the Bragg wavelength shift on the temperature change [2], [4].

$$\lambda_{B,N}(T) = \lambda_{B,0} + \xi * \Delta T_N \qquad (2.1.2)$$

where $\lambda_{B,0}$ is the reference Bragg wavelength, according to which the changes in temperature is calculated, ξ is the thermal sensitivity coefficient, which is approximately 10.2 pm/˚C and ΔT_N is the temperature change. By rearranging Equation 2, the variation in temperature can be found. This algorithm was used to develop a MATLAB code to reconstruct the temperature profile based on the changes in the reflected spectrum of an FBG array. The cost of this FBG array is around $100. However, since there are other components, which are required for using this sensor, it is suggested to add the costs of those components as well. This cost for other components will accumulate for around $10,000, which is the cost of an interrogator. The primary disadvantage of this sensor is its spatial resolution, which is limited to 5 temperature change sensing points over the distance of 0.05 m. Compared to the other

temperature change monitoring technologies, the spatial resolution is low. The other two technologies have the spatial resolution of about 2 mm or less.

The next sensor, which is used to detect distributed temperature profile and reviewed in this work, is a CFBG sensor. In this work, the length of the CFBG sensor was 0.015 m. The main difference between an FBG array sensor and a CFBG sensor is the number of points at which the temperature can be measured over the given distance [1], [2], [21]. In the case of an FBG sensor, the temperature can be measured at 5 points over the distance of 0.05 m, while a CFBG sensor is assumed to provide about 100 measurements over the shorter distance of 0.015 m. Therefore, a CFBG sensor can provide a more detailed distributed temperature profile [22], [30], compared to its alternative, an FBG sensor [1], [2], [21], which is an advantage for the CFBG sensor. The working principle of the CFBG sensor, which was used in this work, is more complicated compared the one of the FBG array sensor and is described further. The setup is the same for the CFBG sensor as it is for the FBG array sensor and includes a light source, a spectrometer, a coupler, a fiber-optic sensor and a computer. The software, which is used to record the changes in the spectrum, is the same as well, I-MON. The temperature reconstruction process starts with the data acquisition process during a thermal ablation (TA) experiment. Once the changes in spectrum are saved as a text file on a computer, the temperature reconstruction process is started and is explained further. Initially, the length of the CFBG sensor is discretized into M gratings [2], [27]. These gratings are assumed to behave as uniform gratings, each having the peak wavelength that depends on the grating period and the effective refractive index,

as described in the previous paragraph, Equation 1. This results in a spectrum from all of these gratings as shown in Figure 2.1.5, which is analyzed to reconstruct the temperature profile [2], [4], [27].

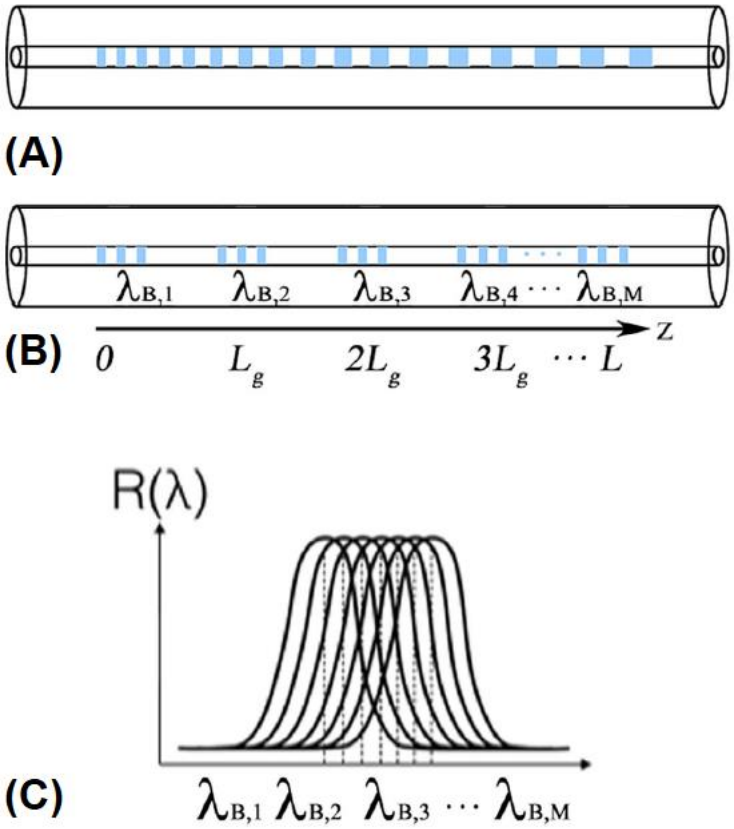

Figure 2.1.5: A model of a CFBG sensor. (A) A CFBG sensor. (B) A model of a CFBG sensor using M uniform FBG sensors. (C) A spectrum combined from M uniform FBG sensors.

The following provides a description of a temperature reconstruction process using a CFBG sensor [2]. In order to obtain the changes in temperature from this sensor, the first step is to obtain a spectrum observed at room temperature, which serves as the reference point. The second step is to simulate a spectrum, which approximates the real one. This is an important step to find the necessary characteristics of the real spectrum. The third step is to start applying temperature to observe changes in the reflected

spectrum. Forth of all, it is required to start finding spectrums, which approximate the real ones. The next step is to find the parameters, which are needed for temperature profile reconstruction. This is achieved by comparing the simulated spectrum to the one, which was constructed using these parameters. Finally, these parameters are used to construct the temperature profile. The necessary equations, in addition to the ones presented in the previous section, are presented below. As can be seen the main idea is to combine the spectrums from all FBGs, which are used to model the one of a CFBG sensor. Equation 3 allows providing the reflected spectrum for each FBG [2], [4]. The transmitted spectrums from all of these FBGs is then combined and converted back to the reflected spectrum, which is shown by Equation 5 [2], [4].

$$R_N(\lambda) = \frac{\sinh^2(L_g\sqrt{k_N^2 - \sigma_N^2})}{\cosh^2\left(L_g\sqrt{k_N^2 - \sigma_N^2}\right) - \frac{\sigma_N^2}{k_N^2}} \tag{2.1.3}$$

$$\sigma_N = \frac{\pi}{\lambda}\delta n_{eff} + 2\pi n_{eff}(\frac{1}{\lambda} - \frac{1}{\lambda_{B,N}}) \tag{2.1.4}$$

$$R_{CFBG} = 1 - \prod_{N=1}^{M}[1 - R_N(\lambda)] \tag{2.1.5}$$

Ones the model is built, the changes observed in the spectrum are treated as variations in temperature along the distance of the sensor. In this work, considering that the main application of temperature sensors is to monitor the temperature change of a tumor that undergoes a thermal ablation process, the most suitable model for temperature profiles is a Gaussian shaped temperature gradient, which makes use of Equation 6 [2], [4].

$$\Delta T(z) = A * \exp(-\frac{(z - z_0)^2}{2s^2}) \quad (2.1.6)$$

where A, z_0 and s are the amplitude, central position and variance respectively. The cost of the CFBG sensor used in this work is around $300 and the cost for other components is the same as for an FBG sensor, which is around $10,000.

Finally, the working principle of a standard fiber connected to an optical backscatter meter is described. In contrast to the previous technologies, this technology provides distributed temperature change monitoring by measuring the Rayleigh backscattering pattern from a standard fiber that is connected to an optical backscatter meter [6], [19]. The Rayleigh backscattering pattern is measured by using the swept wavelength interferometry (SWI) [6]. Figure 2.1.6 shows the system, which is used to conduct these measurements [6].

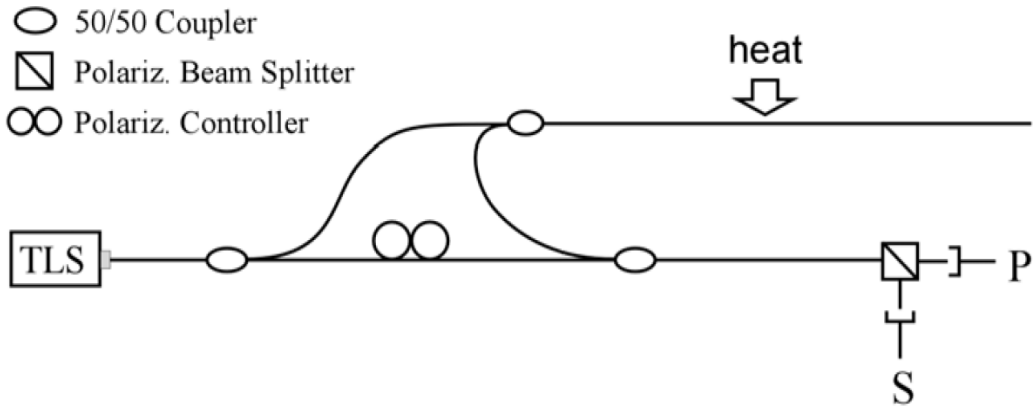

Figure 2.1.6: An optical system used for Rayleigh backscatter measurement

In this Figure 2.1.6, a 50/50 coupler is used to split the light to allow it to pass in both directions, a polarization controller and a polarization beam splitter split the light evenly between 2 orthogonal polarization states [6], [19]. The Rayleigh

backscatter spectrum has an amplitude and a phase, which are measured using the SWI [6]. Having changed the temperature along the sensor, there is a shift observed in the Rayleigh backscatter spectrum [6], [19]. It is claimed that this technology is able to provide temperature change measurements with the accuracy of approximately 0.1 ˚C [7]. The spatial resolution of this technology can be as low as 0.32 mm and the operations are performed in the 1525 – 1610 nm range [7]. However, having such spatial resolution may affect the accuracy of the results. This technology has advantages over the previous two in terms of sensing range, accuracy, and cost of a sensor. However, the main disadvantage of this approach for temperature sensing is the cost of an interrogator, which is used to analyze the data coming from the sensor connected to it. The cost of this interrogator can be 10 times higher compared to the one used for the FBG array and the CFBG sensors.

There are also other technologies, which may be used for distributed temperature change monitoring. For example, Magnetic Resonance Imaging (MRI) can be applied for the chosen application, since it is a non-invasive technology and provides distributed temperature change monitoring. The disadvantage of this technology is its expensiveness. There are also other technologies, such as thermocouples. However, most of such technologies do not provide distributed temperature monitoring and only measure temperature at one point, which is not suitable for the chosen application.

2.2 Thermal Ablation Technologies

In this work, it is suggested to focus on one application, which is minimally invasive thermo-therapies in cancer care. In particular, the procedures that involve thermal ablation of liver tumor is studied. The objective of using fiber-optic sensors in this particular application is to make sure that cancer cells are removed, while the damage of healthy cells is minimized during a thermal ablation process. In thermal ablation, the necrosis of cancer cells is achieved by heating them to a certain degree for a specific period of time [28]. Consequently, it is required to consider both applied temperature and exposure time for the successful necrosis of cancer cells. In [8], it is claimed that by applying the temperature of 52˚C for 60 seconds will result in the necrosis of cancer cells, and at 60˚C, this process is instantaneous. Therefore, considering minimal invasiveness of the fiber-optic sensors, which are studied in this work, it may be useful to employ them for monitoring changes in temperature of the treated tissue in thermal ablation procedures. However, there are limitations, which need to be considered as well for this particular application. One of the most significant ones is that a sensor is also sensitive to strain effects, which means that if a sensing region of an optical fiber bends or experiences pressure, the process of reconstructing a temperature profile may be affected. Therefore, in this work, when running thermal ablation experiments, the fiber-optic sensors were properly placed by minimizing the effects of strain. However, in real clinical settings, a patient's breathing may cause unnecessary strain effects. Therefore, it is important to find a method for minimizing

the effects of strain in real clinical settings. This issue may be solved with the help of a catheter, which will be described in more details in the following chapters. In addition, the fiber-optic sensors are made from glass and are fragile. Though it is unlikely that a sensor breaks as a result of thermal ablation procedures, it is still important to prevent the sensors from breaking. This can also be accomplished with the help of a catheter, which is described in the following chapters.

Some of the most popular techniques for thermal ablation include laser ablation (LA), microwave ablation (MWA), radiofrequency ablation (RFA) and high intensity focused ultrasound (HIFU) ablation. This work includes the experiments that involved the RFA of a beef liver and the HIFU ablation of a fibroadenoma, both of which were conducted ex-vivo. These two minimally invasive techniques for thermal ablation are described in this section.

RFA is mainly used for thermal ablation of livers and kidneys, [15]. This technology makes use of the current coupling to a tissue, where an RF probe was placed. This probe is made from metal, most part of which is insulated, and only the tip of this probe serves as a conductor, and it is used to transfer the heat to the tissue. The voltage is produced between the tip of the probe and the ground; as a result, the area between these two electrodes is where the electrical field is produced [9]. In cancer care, it is typical to set the frequency range to less than 1 MHz, since it allows the current to move having a velocity, the value of which is dependent on the intensity of the electrical field [9], [10]. There are advantages of using this technology, which is the possibility of expanding the area of ablation by using multi-probes. However, there

is a limitation of using RFA, which is concerned with placing an RF probe inside a human body; therefore, there is a change for bacteria to infect the body [9], [10].

It is also important to review another type of ablation, HIFU ablation, which is primarily used for removing tumors in kidneys, livers, breasts, prostates and other organs [11], [12]. The working principle of HIFU is based on the oscillatory movements of a piezoelectric crystal, which creates ultrasound waves. The power density delivered to a target position varies from 100 to 10000 W/cm^2 [12]. The tissue that is treated using HIFU is damaged as a result of heat transfer. There is a limitation, which needs to be carefully considered, before performing the HIFU ablation process and that is an energy deposition. If the HIFU beam is not properly focused and the target is moving, the procedure may not provide the necessary results.

There are other common alternative thermal ablation technologies, which are used for tumor removal, which are LA and MWA. The LA technology is based on the process of absorbing the laser light by a tissue, which results in the increase of the temperature of this tissue [20]. It is common to use 980 nm and 1064 nm wavelengths for the LA processes in cancer care [13]. At these wavelengths, an optimal absorption of light is observed. This technology is commonly used for removing tumors in livers, prostates and others. Another technology for thermal ablation is MWA. This technology is based on the frictional energy, which is produced as a result of polar water molecules interacting with the electromagnetic field. This energy is then transferred into heat. MWA technologies commonly operate in 915 MHz - 2.45 GHz

range and the maximum power delivered to a tissue is 100 W [14]. This technology was used for removal of lung and liver tumors. There is also an alternative to thermal ablation, which is to remove a tumor using surgical methods; however, it may not be suitable for various scenarios and may result in healthy cells being damaged.

Chapter 3 – Description of Conducted Work

There were a number of tasks, which involved designing and conducting thermal ablation and other experiments using fiber-optic sensors, obtaining thermal maps using MATLAB, analyzing results and providing suggestions on how to improve the whole process. This chapter is split into 3 sections. The first section explains the procedures for the comparison of the temperature sensing technologies based on the CFBG, the OBR, and the 5-element FBG array during an RFA experiment. These 3 fiber-optic sensing technologies were compared to find the most suitable one for the given application, which is using the temperature sensor for minimally invasive thermo-therapies. These 3 technologies were used in one experiment at the same time to compare and evaluate their performance. The conclusion is that, considering the criteria listed above, all of these sensors are good candidates for temperature change monitoring in minimally invasive thermo-therapies; however, the most suitable one is the CFBG sensor. The next section focuses on the application of the 5-element FBG array during a HIFU experiment conducted in clinical settings. Finally, the work conducted to analyze the effects of catheterization is presented.

3.1 Design and implementation of an RFA experiment for the comparison of the distributed temperature sensors based on CFBG, OBR, and 5-element FBR array

Since it was required to compare 3 temperature sensing technologies, which were based on the 5-element FBG array, the CFBG and an optical backscatter meter, an RFA experiment was conducted. First of all, all of these 3 sensors were gathered and checked for their operability. The 5-element FBG array was connected to the interrogator, and the software, I-MON, was used to observe the reflected spectrum from this sensor. The same procedure was applied for the CFBG sensor. Additionally, the experiment was designed such that these 3 sensors are used simultaneously during the same RFA experiment. Therefore, it was required to select suitable 5-element FBG array and CFBG sensors, which can be used by one interrogator at the same time. This was done with the help of a coupler, which allowed the light to be transferred from the light source to the 5-element FBG array and CFBG sensors simultaneously, Figure 3.1.1. Also, the reflected spectrum was monitored by the same software, I-MON, which meant that any overlapping of the reflected spectrum from these 2 sensors would have made it indistinguishable from each other and impossible to reconstruct. Therefore, these 2 sensors were operating at different wavelength ranges, considering their

multiplexing capabilities [25]. The 5-element FBG array sensor was operating in 1.565 – 1.575 nm, while the CFBG sensor was operating in 1.53 – 1.56 nm. These values indicate that there was no overlapping of the reflected spectrum of these 2 sensors. The length of the CFBG sensor was 0.015 m, while the length of the FBG sensor was 0.05 m. Also, the standard fiber was connected to an optical backscatter meter. It was observed that the temperature variations were recorded along the whole length of the standard fiber and that it was suitable for running an RFA experiment. The second step was to check the operability of the RFA machine, namely Leanfa Hybrid Generator, and find the appropriate value of applied power, which ensures slow propagation of heat into the tissue. After running an experiment on a piece of a beef liver, it was decided to set the value of power to 30 W. Third of all, the experimental setup was prepared, as shown in Figure 3.1.1.

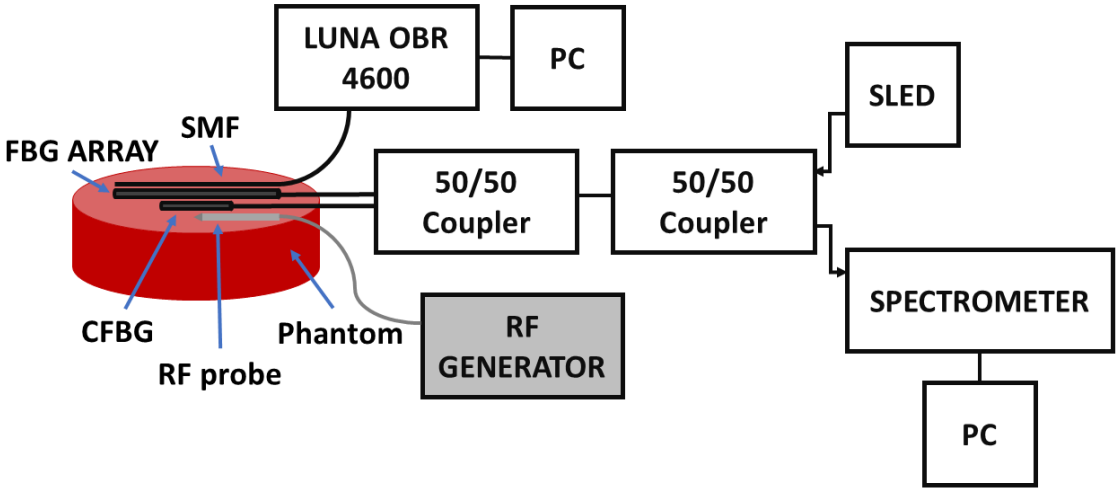

Figure 3.1.1: The schematic of the experimental setup for the RFA of the liver beef with three sensors: the FBG, the CFBG and the standard fiber connected to an optical backscatter meter

As can be seen from Figure 3.1.1, the setup involved all 3 sensors and the necessary equipment to record the changes in spectrum. In case of the standard fiber connected to an optical backscatter meter, the software also showed the changes in temperature, which means that no additional operations in MATLAB were necessary, expect for detecting the thermal maps, which were obtained using MATLAB. For the 5-element FBG array and CFBG sensors, an additional coupler was added, so that one interrogator could record the values from both of these sensors. The final experimental setup is shown in Figure 3.1.2.

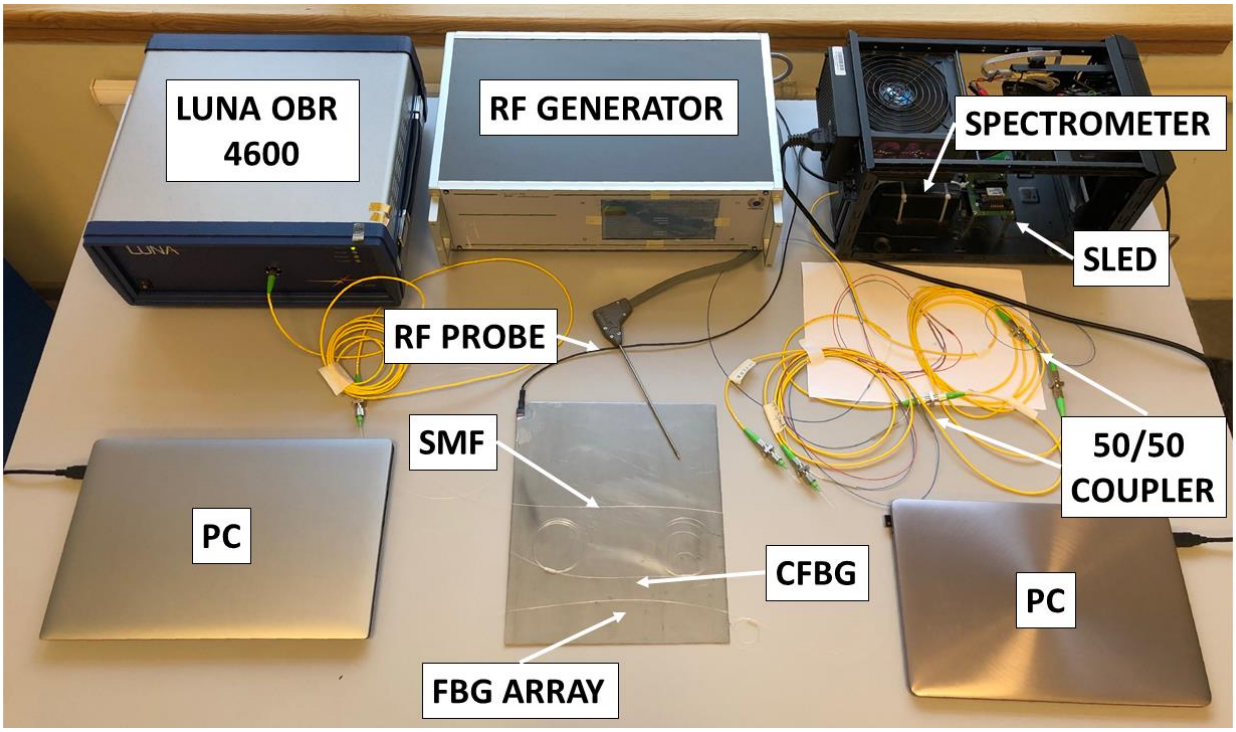

Figure 3.1.2: The experimental setup for the RFA of the liver beef with three sensors: the FBG, the CFBG and the standard fiber connected to an optical backscatter meter

The forth step was to properly locate the sensors and the RF probe on a piece of beef liver. The RF probe is used to transfer the heat to the tissue. By turning on the RFA machine and indicating the amount of power supplied, there is a certain amount

of heat being delivered to the tissue using the RF probe. The sensors were linked together and placed between the two pieces of liver, while the RF probe was placed perpendicular to these sensors. Finally, the experiment was conducted, and the necessary data was obtained. The temperature reconstruction process was conducted in MATLAB using the theoretical background presented in Section 2.1. The results are shown in the next chapter, Section 4.1.

3.2 Preparation of the experimental setup and implementation of the HIFU ablation experiment conducted in clinical settings using a 5-element FBG array

Also, another experiment was conducted with the 5-element FBG array, which showed that the 5-element FBG array can be used as a distributed temperature sensor in HIFU ablation experiments in clinical settings. The length of the sensor was 0.05 m with the spatial resolution of 0.01 m, and it was operating in the range from 1.565 nm to 1.575 nm. The HIFU ablation experiment was conducted on a fibroadenoma in clinical settings. Initially, the 5-element FBG array sensor was connected to the interrogator and placed inside the fibroadenoma, which, in turn, was placed inside the HIFU equipment. The next step was to turn on the HIFU machine and start gathering

the data using the interrogator. Finally, once the data was collected, the temperature reconstruction process was conducted in MATLAB. Figure 3.2.1 (A) shows the experimental setup for the HIFU ablation experiment, while Figure 3.2.1 (B) shows the HIFU console, which was used to observe the changes of the tissue and the placement of the fiber-optic sensor. The supplied powered varied from 220 to 400 W, which can be observed in the results section, Section 4.2.

(A)

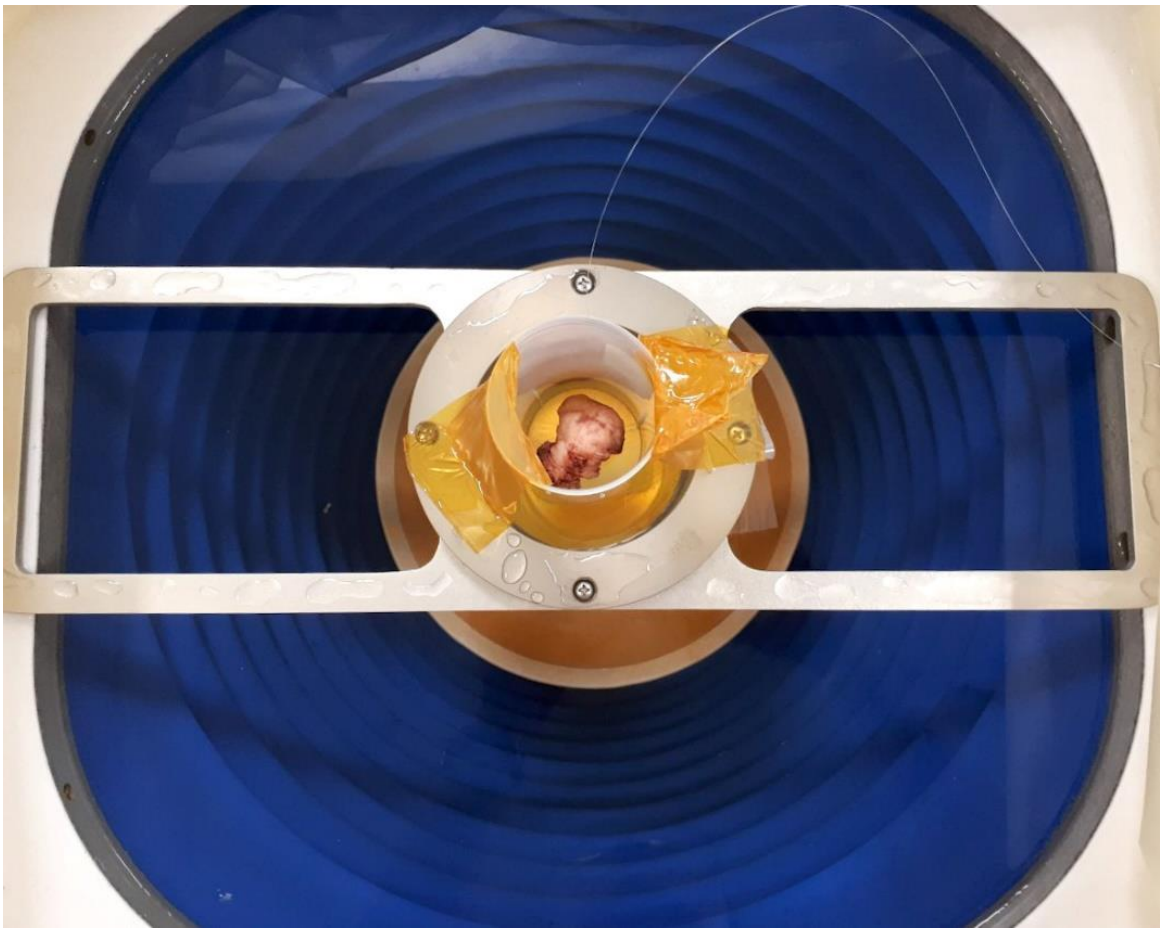

(B)

Figure 3.2.1: (A) The experimental setup for the HIFU ablation of the fibroadenoma using the FBG sensor that showed the effect of strain, (B) The HIFU console used in the HIFU ablation experiment

Figure 3.2.2 shows the schematic of the experimental setup for the HIFU ablation experiment on a fibroadenoma using the 5-element FBG array sensor. The results showed that the 5-element FBG array sensor can be used in HIFU ablation experiments in clinical settings. In addition, considering that in clinical settings there may be effects of strain, as a result a patient's breathing or slight movement, it is

required to minimize them using a catheter. The analysis of the effects of a catheter to for minimizing the effects of strain are provided in the next chapter, Section 4.2.

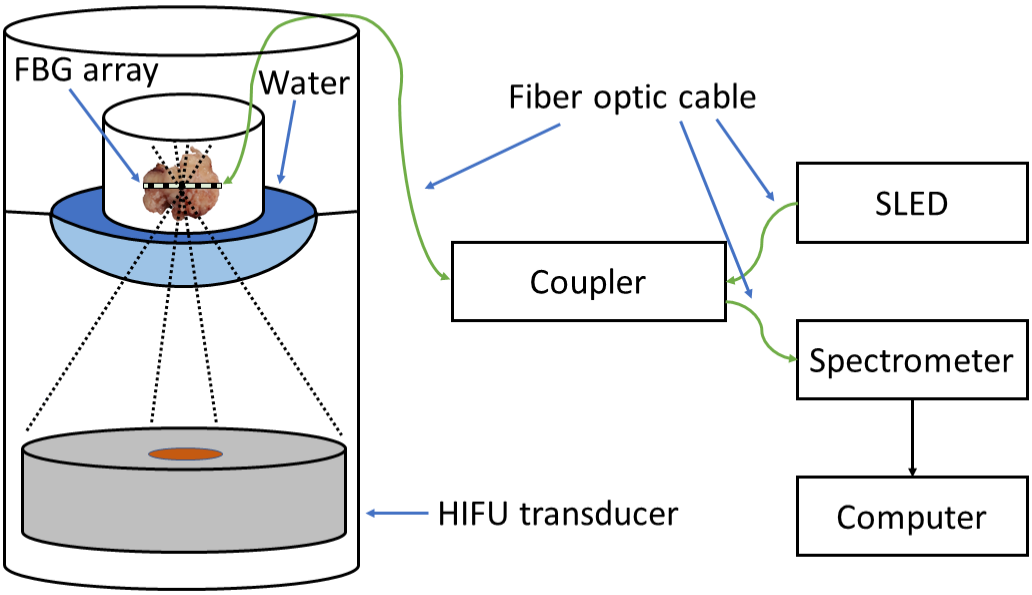

Figure 3.2.2: The schematic of the experimental setup for the HIFU ablation of the fibroadenoma using the 5-element FBG array sensor that showed the effect of strain

3.3 Design and implementation of the experiment to analyze the effects of catheterization

Considering that the strain effects have negative effects on the temperature reconstruction process, it is important to minimize them. It was proposed to conduct the further thermal ablation experiments using a catheter. By placing a sensor inside of

a catheter, the effects of strain, which exist as a result of a tissue expansion or a patient's breathing, are minimized. It was decided to use the Chiba Biopsy Needle (22 gauge) as a catheter for this specific application. It was required to also run the experiments to analyze the effects of a catheter on the temperature readings of a fiber-optic sensor. There were 2 experiments conducted to analyze the effects of a catheter on the temperature change monitoring by monitoring the differences in temperature change readings from the sensors, one of which was placed inside of the catheter, as shown in Figure 3.3.1. The first experiment was conducted with the help of a plastic bag, in which warm water was poured, Figure 3.3.2. By placing the plastic bag with warm water on top of the sensors, the temperature change was expected to be similar. The results are presented in the next chapter, Section 4.3.

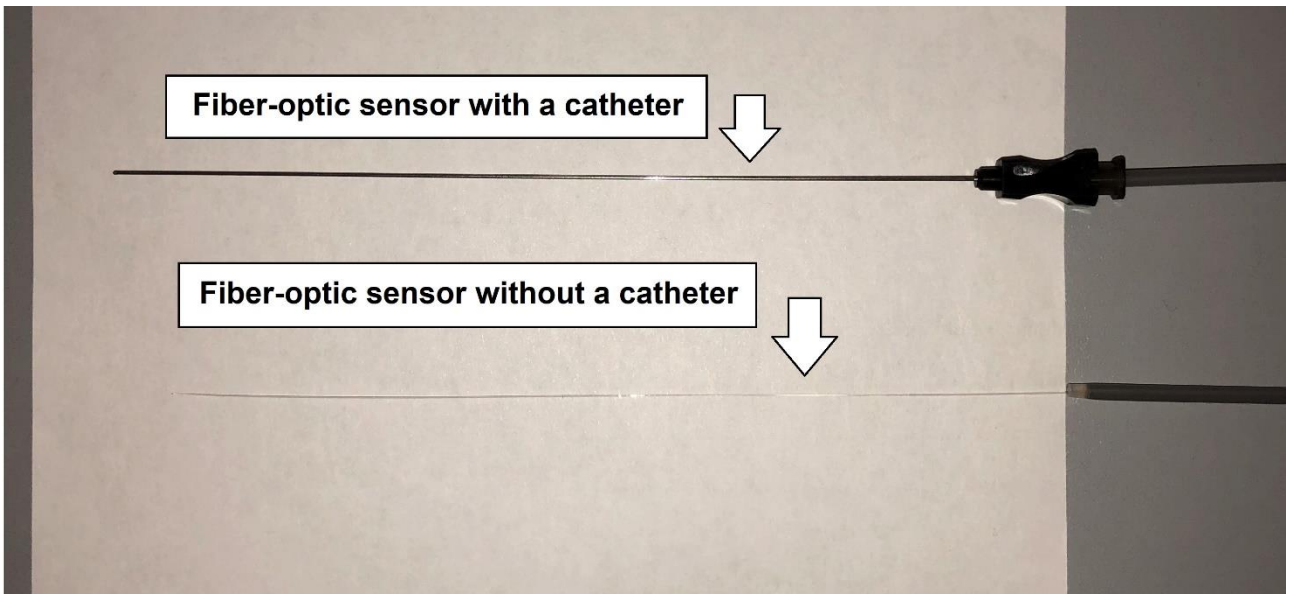

Figure 3.3.1: The experimental setup with the fiber-optic sensors, one of which is placed inside of a catheter (22 gauge), to observe the effects of a catheter on the temperature change

Figure 3.3.2: Placing a plastic bag with warm water on top of the fiber-optic sensors to observe the effect of a catheter on the temperature change

The second experiment was conducted using a piece of a beef liver. The experimental setup included a standard fiber, an optical backscatter meter, a coupler, an RFA machine and a beef liver. Figure 3.3.3 shows the experimental setup for this experiment. Once all components were connected, the sensors were placed at approximately equal distance from the RF probe, which was used to transfer the heat to the piece of a beef liver. It was expected to observe a similar temperature change for both of these sensors. The results are shown in the next chapter, Section 4.3.

Figure 3.3.3: The experimental setup for analyzing the effect of a catheter on the temperature change

Chapter 4 –Results and Discussion

4.1 Comparison of the distributed temperature sensors based on CFBG, OBR, and 5-element FBR array

The first experiment was conducted to compare 3 temperature change sensing technologies using the RFA machine, involving the temperature sensors based on the 5-element FBG array, the CFBG and the standard fiber connected to an optical backscatter meter. The experimental setup, as well as the schematic, were both shown in the previous chapter, Section 3.1. The results were obtained after the data was collected and the processing of the data to complete the temperature reconstruction process took 10 seconds to process ~260 spectral measurements for the 5-element FBG array sensor, while for the CFBG sensor, this process took 81 seconds for the same amount of spectral measurements. Considering that the time it took to collect the data was about 260 seconds, it is clear that the time required to process this data is significantly less, which indicates that both of these sensors are operating in real-time. The temperature reconstruction was conducted in MATLAB and the theoretical background required for the temperature reconstruction process for both of these sensors was provided in Section 2.1. As for the OBR technology, the OBR software is used for the temperature reconstruction and takes ~ 1 second for each spectral

measurement. The results showed that the increases and decreases of temperature were precisely detected by all 3 sensors. For the first ~ 220 seconds, the temperature was increasing, and all 3 sensors detected the changes in temperature, and, once the temperature started decreasing, which started at ~ 220 second, the decrease was precisely detected by all 3 temperature sensors. The area of ablation required for the analysis was represented with the distance of 0.015 m from the peak temperature to the lowest temperature readings, which can be seen in Figures 4.1, 4.2 and 4.3. An additional observation is based on the fact that the length of the CFBG sensor is 1.5 cm, which does not provide the full temperature profile of the tissue that was thermally ablated, Figure 4.1. In contrast, the sensing technologies, which are based on the 5-element FBG array and the OBR technology, provide full temperature profile, which is achieved as a result of having larger temperature sensing ranges. The sensing range for the 5-element FBG array is 5 cm, while for the OBR technology, the sensing range is limited to the length of the standard fiber connected to it, which exceeds 40 cm in this particular experiment. For the representation of the results from the OBR, the length of the sensing range was limited to 4 cm, which fully represents the thermally ablated region of the tissue. The results were presented on Figures 4.1.1, 4.1.2, and 4.1.3, as the contour maps, and the value of 0 on the y-axis indicates the maximum temperature readings observed for the given distance along the sensor.

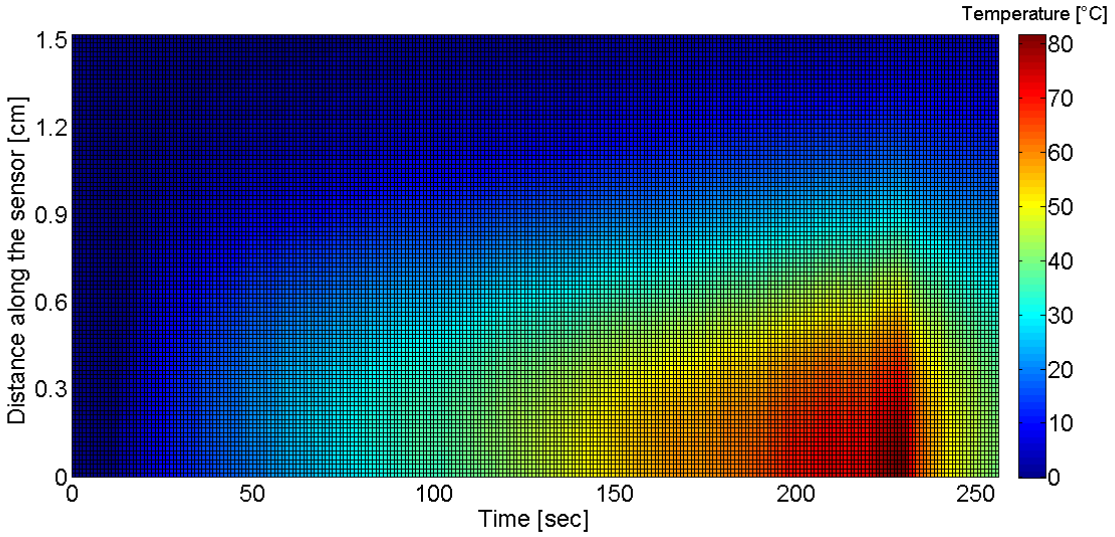

Figure 4.1.1: The temperature change detected in the RFA experiment on the beef liver using the CFBG sensor

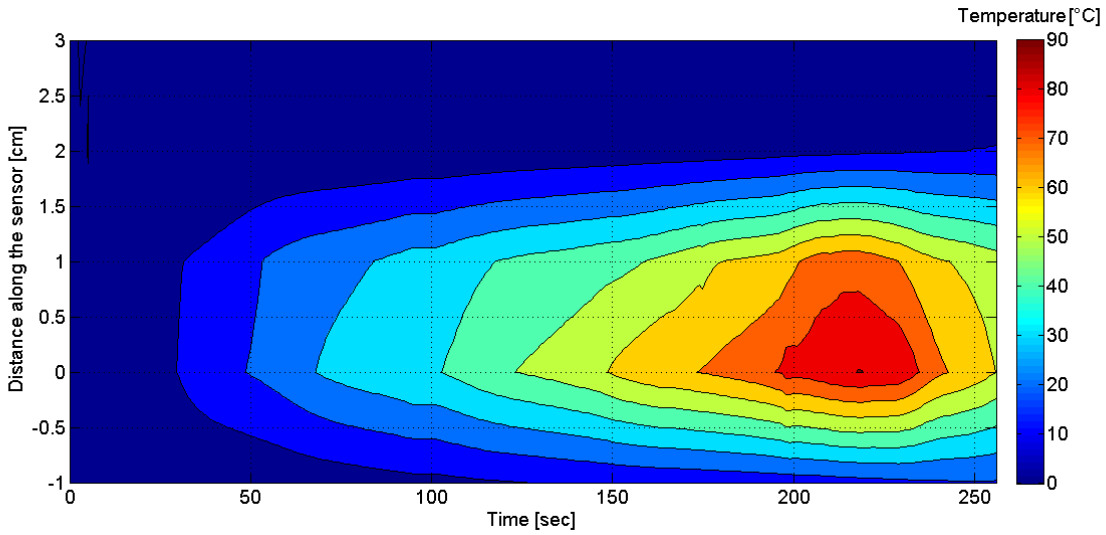

Figure 4.1.2: The temperature change detected in the RFA experiment on the beef liver using the FBG sensor

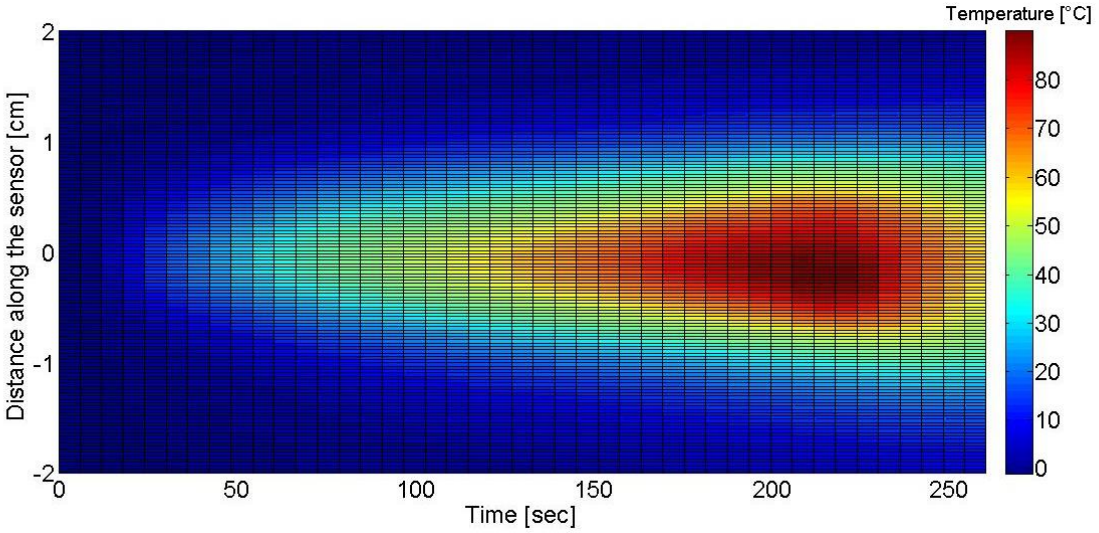

Figure 4.1.3: The temperature change detected in the RFA experiment on the beef liver using the standard fiber connected to an optical backscatter meter

These 3 fiber-optic temperature sensing technologies were compared based on the maximum achieved temperature change over time, which is shown in Figure 4.1.4. First of all, it should be mentioned that when conducting experiments, the data acquisition process could have started with a delay for the OBR technology, which may explain the fact that the temperature change observation starts slightly earlier for the 5-element FBG array and the CFBG sensors. However, it can be seen that the peak temperature readings achieved by the sensors based on the OBR and the 5-element FBG array are approximately equal at ~ 90˚C. Also, it can be seen that by comparing the temperature change readings from the 5-element FBG array and the CFBG sensors, the changes in temperature, such as increases and decreases, are in accordance to each other, Figure 4.1.4. For example, in Figure 4.1.4, the temperature change process starts at the same time for both sensors; at ~ 100 seconds, the temperature is constant for both of these sensors; at ~ 225 seconds, there is a significant decrease recorded by both

sensors. However, the temperature readings from the CFBG sensor are different in value to the ones from the 5-element FBG array sensor, which are, in turn, are closer to the ones from the sensor connected to the OBR. The difference in temperature readings from the CFBG sensor can be explained by the limited temperature sensing range, which is 1.5 cm, and, therefore, may not represent the full temperature profile, omitting the peak temperature achieved by the sensor. Another reason is improper placement of the sensors during the RFA experiment, the sensors could have moved slightly during the experiment, and, considering the heterogeneity of the tissue and heat acquisition, there could have been differences in the temperature readings. Finally, the temperature coefficient claimed by the manufacturer of the CFBG sensor is 10.2 pm/˚C; however, this value may have been altered. Considering that the temperature coefficient is crucial in the temperature reconstruction process, it may explain the differences in temperature readings of the CFBG sensor.

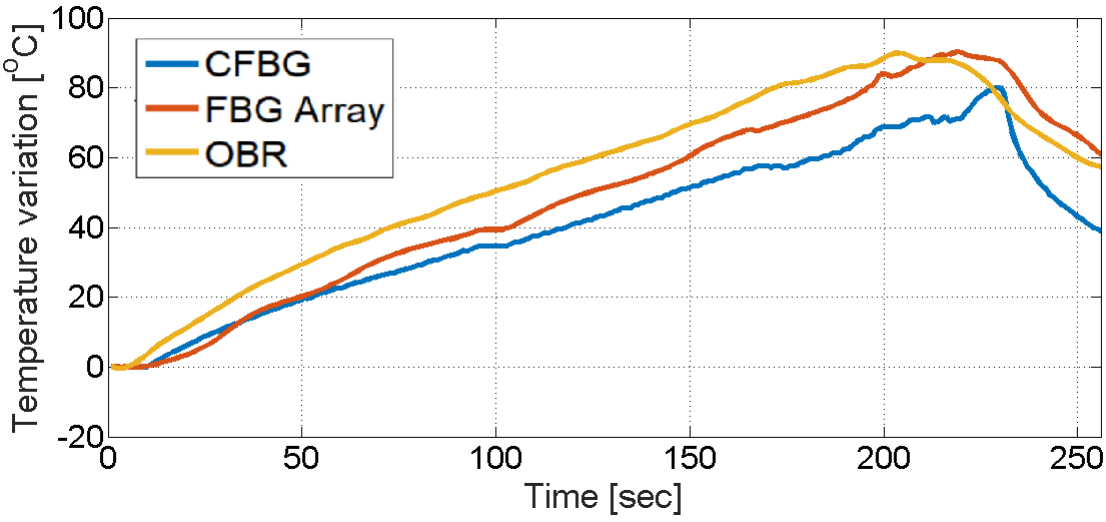

Figure 4.1.4: The comparison of the maximal temperature change over time for the temperature sensors based on CFBG, 5-element FBG array, and OBR

The 3 fiber-optic temperature sensing technologies were also compared based on the temperature variation as a function of the distance along the sensor at various instances of time, which is shown in Figures 4.1.5, 4.1.6, 4.1.7, 4.1.8, and 4.1.9. The time instances are at 15, 65, 115, 165, 215 seconds, which are respectively shown in Figures 4.1.5, 4.1.6, 4.1.7, 4.1.8, and 4.1.9. It was decided to compare these sensors having the maximum value achieved by the sensors at the center and observing the gradual decrease of the temperature on the sides of the sensors. According to Figure 4.1.5, the temperature variation of the CFBG-based and the OBR-based sensors are close to each other over the given distance with the maximum temperature difference of 1˚C between the two sensing technologies. The 5-element FBG array sensor was reconstructed using a splice function, which is used as a result of having only 5 temperature sensing points over the sensing range of 5 cm of this sensor.

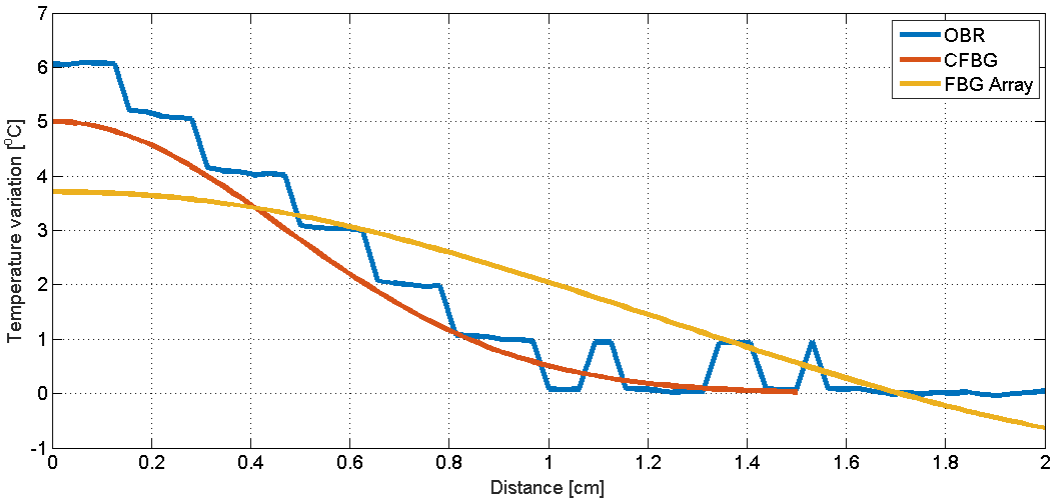

Figure 4.1.5: The comparison of the temperature variation as a function of the distance along the sensor at 15 seconds for the temperature sensors based on CFBG, 5-element FBG array, and OBR

The shapes of the temperature variation of the CFBG-based and the OBR-based temperature sensors as a function of distance are similar for the time instances of 15, 65, 115, 165 and 215 seconds. However, the temperature readings of the OBR-based sensor exceed the ones of the CFBG-based sensor. This could be explained by the possibility of having an altered temperature coefficient of the CFBG sensor and improper placement of the sensors during the experiment, and, since the sensors are also subject to the changes in strain, the effects of strain could have also affected the experimental results. Considering the heterogeneity of the tissue, which was a piece of a beef liver, the tissue, where the sensors were placed may be subject to shrinking and may result in tension on one of the sensors. Therefore, for the future experiments, it is recommended to minimize the effects of strain by using a catheter. There were also a number of experiments with a catheter conducted to analyze the effect of a catheter on the temperature reconstruction process. For the 5-element FBG array sensor, a detailed temperature profile cannot be achieved due to its low spatial resolution. The spline function was used in MATLAB to approximate the temperature profile from this sensor; as a result, the shape of the temperature variation as a function of distance does not fully coincide with the lines observed from the other 2 sensors. The reason for this is the spatial resolution of the 5-element FBG array, which provides only 5 measurement points over the distance of 5 cm. It is recommended for the future experiments to increase the spatial resolution of this sensor by placing several of them in parallel to each other considering the measurement points of each and making sure that they do not coincide. As a result, by having 2 of 5-element FBG arrays, the spatial

resolution is increased to 10 measurement points over the distance of 5.5 cm. In addition, if 3 of 5-element FBG arrays are used, the spatial resolution is increased to 15 measurement points over the distance of approximately 5.75 cm.

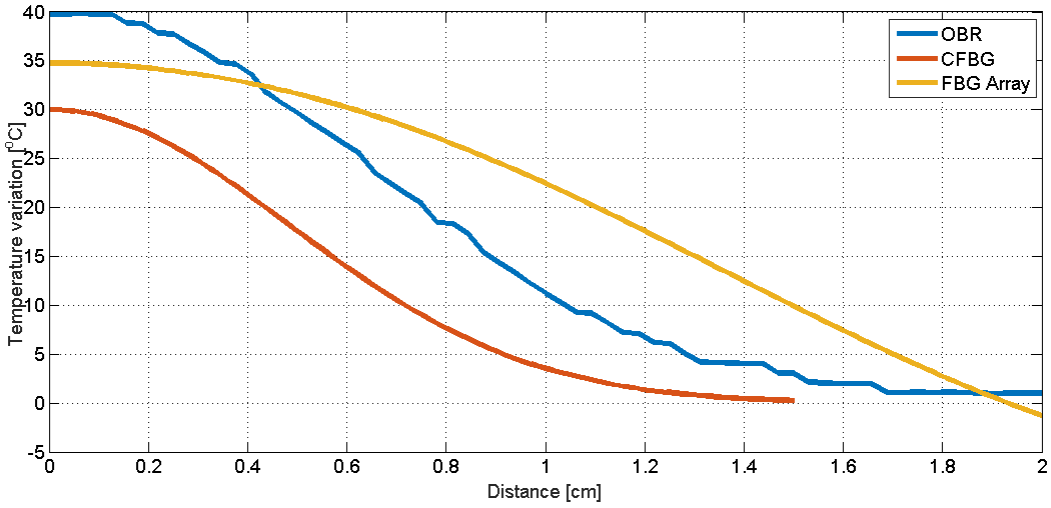

Figure 4.1.6: The comparison of the temperature variation as a function of the distance along the sensor at 65 seconds for the temperature sensors based on CFBG, 5-element FBG array, and OBR

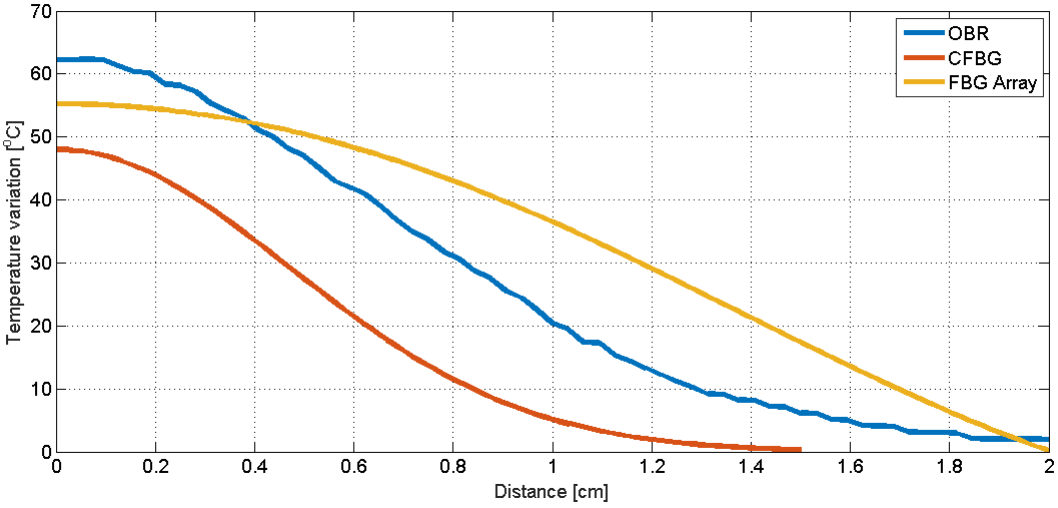

Figure 4.1.7: The comparison of the temperature variation as a function of the distance along the sensor at 115 seconds for the temperature sensors based on CFBG, 5-element FBG array, and OBR

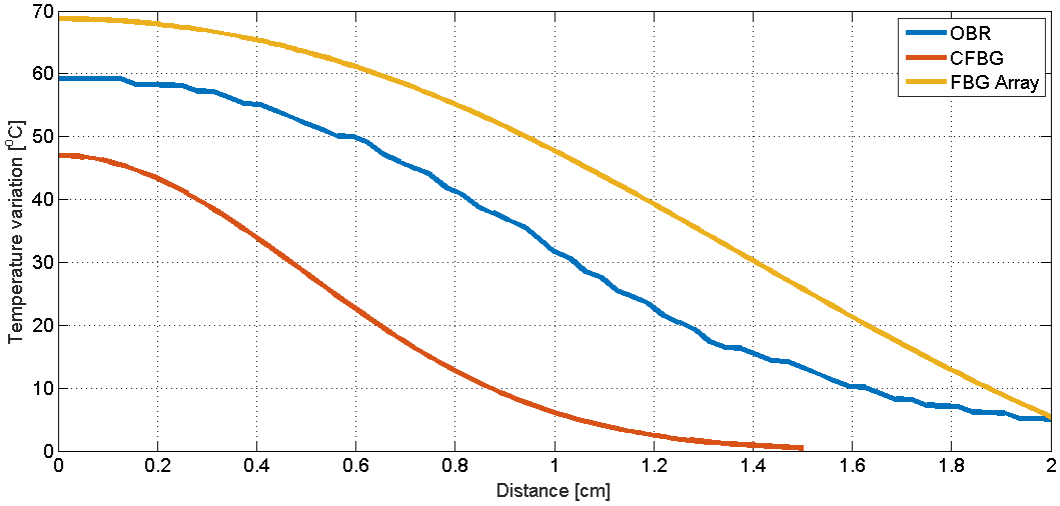

Figure 4.1.8: The comparison of the temperature variation as a function of the distance along the sensor at 165 seconds for the temperature sensors based on CFBG, 5-element FBG array, and OBR

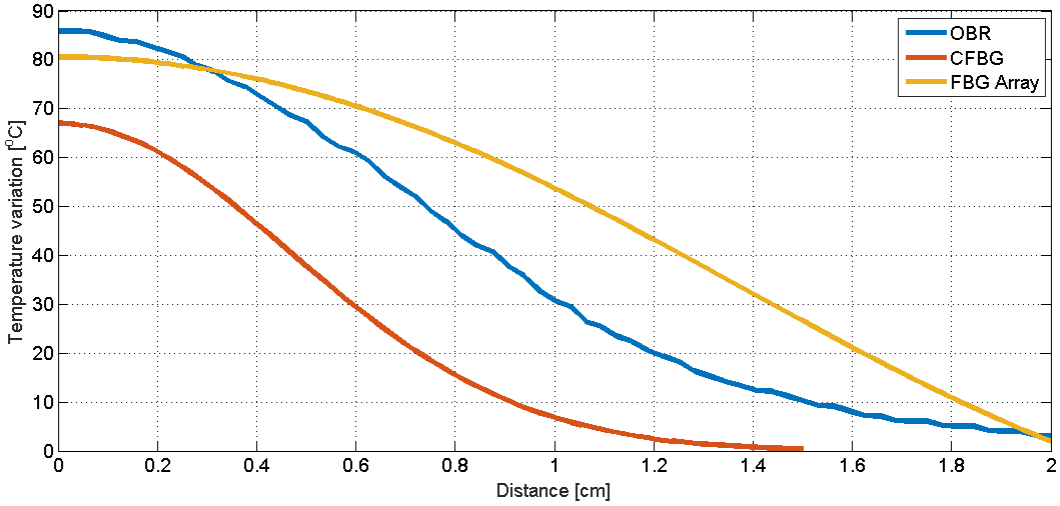

Figure 4.1.9: The comparison of the temperature variation as a function of the distance along the sensor at 215 seconds for the temperature sensors based on CFBG, 5-element FBG array, and OBR

Considering the application of these sensors, which is minimally invasive thermo-therapies for cancer care, it is required to achieve the temperature of 60 ˚C, which corresponds to the temperature of immediate removal of cancer cells. In Figure 4.1.9, it can be seen that the extension of the tissue exposed to the 60 ˚C is 0.5 cm, 0.9 cm, and 1.25 cm for the sensors based on the CFBG, the OBR, and the 5-element FBR array respectively, taking into account the room temperature of 21 ˚C, which adds up to the temperature reading on the y-axis. Based on the characteristics of the sensing technologies, it can be stated that the 5-element FBG array is lacking the necessary spatial resolution for the given application, which can be improved given the recommendations stated previously are fulfilled. The cost of the OBR interrogator required can exceed the cost of the interrogator for the other 2 sensors by as much as 10 times. To summarize, there are a number of limitations in this experiment, which include the inconsistency in the temperature coefficient values set by the manufacturer. This value was set to 10.2 pm/˚C, which in actuality may be different. In addition, the sensors were located inside the beef liver close to each other; however, there was a chance for these sensors to move slightly, which may have resulted in the difference of these temperature readings. Also, the heterogeneity of the tissue could have resulted in the strain effects. Table 4.1.1 summarizes the characteristics of the temperature sensors used in this experiment. It can be seen that the time required to reconstruct the temperature profile for all of the sensors is less or equal to the time needed to acquire the data, which means that the sensors operate in real-time. The spatial resolution is low for the 5-element FBG array, which is 1 cm, while for the CFBG sensor it is less

than 1 mm. The spatial resolution of the CFBG sensor is more suitable for minimally invasive thermo-therapies, since it provides more details. The spatial resolution achieved using the OBR technology is ~ 1-2 mm, which is also suitable for the given application of minimally invasive thermo-therapies. The hardware setup is identical for the 5-element FBG array and the CFBG sensors, considering that the same interrogator is used in the data acquisition process. The OBR interrogator is similar to the one used with the 5-element FBG array and the CFBG sensors, in a sense that it is also connected to a fiber-optic sensor and a computer. However, a different software is used, which is the OBR software. However, this interrogator is significantly heavier and is not as portable as its alternative. Further improvements of the interrogator built for the 5-element FBG array and the CFBG sensors could be made. For example, the size of the box can be reduced and the light emitting source can be replaced with a more compact one [29]. The temperature sensing range is the highest for the standard fiber connected to the OBR, and it is the lowest for the CFBG sensor. The 5-element FBG array sensor provides the sensing range of 5 cm; however, since the spatial resolution is only 1 cm, it is more advantageous to use the CFBG-based or the OBR-based sensing technologies. Finally, the cost of the sensor combined with the cost of the interrogator for the OBR-based sensor is approximately 10 times more compared to the one of the CFBG or the 5-element FBG array sensors. Therefore, taking into account the characteristics of the sensors and the recommendations for conducting future experiments, it is suggested that the CFBG sensor is the most advantageous compared to the other 2 sensing technologies. For future experiments, the primary

recommendations are to use a CFBG sensor with the length of 5 cm, which is suitable for detecting the temperature change of the ablated region of a larger scale, and to calibrate the CFBG sensor to get to know if the temperature coefficient has been altered compared to the value claimed by the manufacturer. Also, it is suggested to use a catheter to minimize the effects of strain.

Table 4.1.1: Comparison of the temperature sensors based on CFBG, OBR, and 5-element FBG array

	Chirped FBG	5-element FBG array	Standard fiber connected to an optical backscatter meter
Cost of the sensor	$300	$100	$35
Cost of the interrogator	$10,000	$10,000	$100,000
Time for reconstructing the temperature profile for the acquired 260 spectral measurements (260 seconds)	81 sec	10 sec	1 second for 1 measurement
Spatial resolution	< 1 mm	1 cm	1-2 mm
Sensing range	1.5 cm	5 cm	Along the whole distance of the standard fiber

4.2 HIFU ablation experiment conducted in clinical settings using a 5-element FBG array as a distributed temperature sensor

Another experiment was conducted using the HIFU ablation machine and the 5-element FBG array sensor on a fibroadenoma in clinical settings. The experimental setup was described in the previous chapter, Section 3.2. As can be seen from Figure 4.2.1, the temperature change was recorded using a 5-element FBG array sensor. The heating process was conducting by supplying the power from 220 to 400 W. It can be seen by observing the peaks that the heating process was not continuous, but rather discrete, Figure 4.2.1. In Figure 4.2.2, it can be seen that during the HIFU ablation process by applying the power of 220 and 400 W (maximum temperature peaks), the heating is almost instantaneous, while the cooling of the tissue is exponential. In case of the results shown in Figure 4.2.3, it can be seen that the thermally-ablated region is the region where the change of color can be visually-observed, which means that the heat was transferred to the tissue. Considering that this experiment was conducted in clinical settings, there may be the effects of strain and it is important to address this issue. The effects of strain can be minimized with the help of a catheter, which is described in the next section, Section 4.3. Overall, it was shown that the 5-element FBG array sensors can be applied in the HIFU ablation experiments. One of the

recommendations may be to use several 5-element FBG arrays in the next HIFU ablation experiment to increase the spatial resolution of the sensing region.

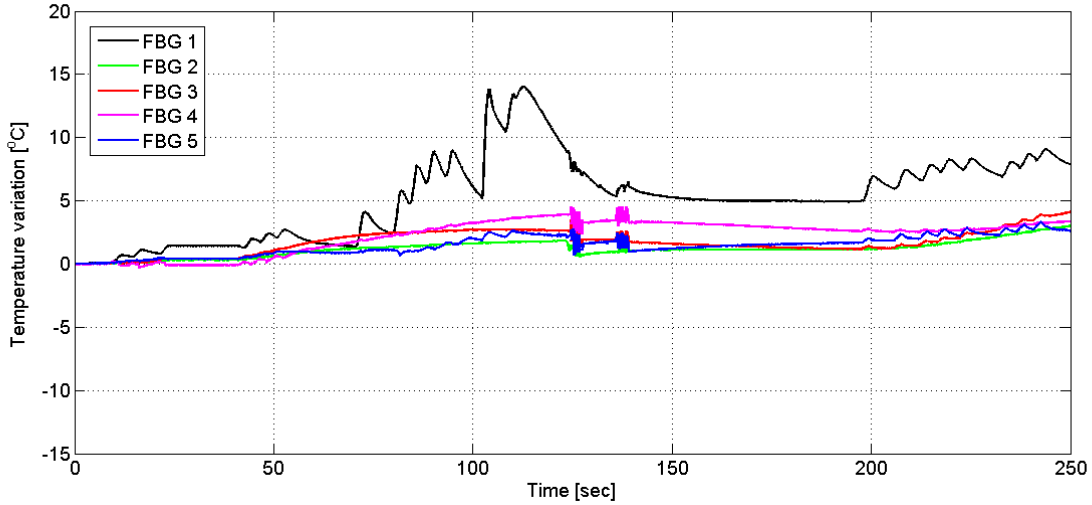

Figure 4.2.1: The effects of strain detected by the FBG sensor in the HIFU ablation experiment conducted in clinical settings

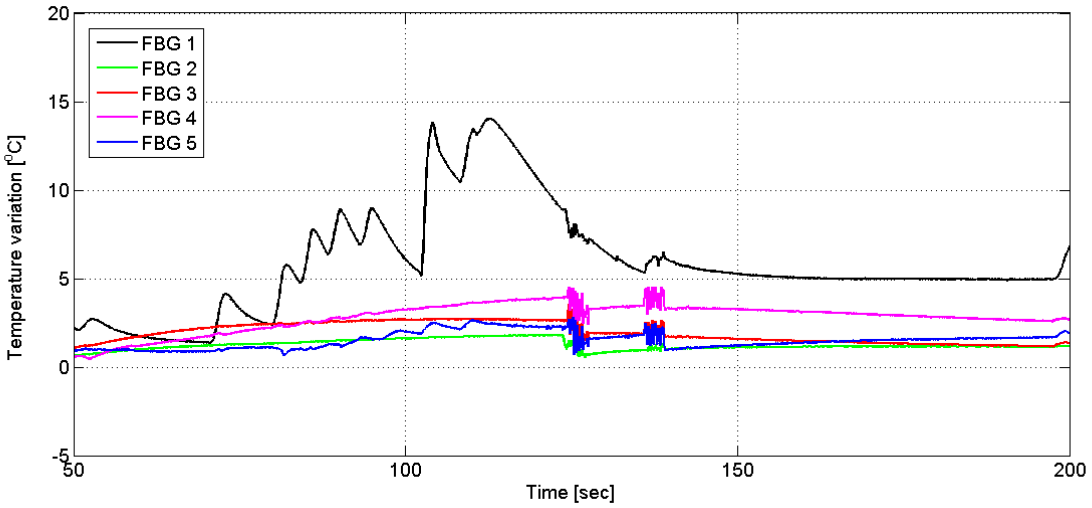

Figure 4.2.2: The instantaneous increase in temperature and the exponential cooling of the tissue in the HIFU ablation experiment conducted in clinical settings

Figure 4.2.3: The thermally-ablated region of the fibroadenoma after the HIFU ablation process

4.3 Analysis of the effects of a catheter on the temperature reconstruction process and minimization of the effects of strain using this catheter

It was suggested to use a catheter in conducting thermal ablation experiments. The main idea is that a sensor is placed inside a catheter; as a result, the effects of strain are minimized in the sensing region area. Section 3.3 provides the detailed information on the preparation of the experimental setup. First of all, the experiment was conducted by placing a plastic bag with warm water poured in it on top of the fiber-optic sensors, one of which is inside the catheter, the Chiba Biopsy Needle (22 gauge). The experiment was conducted to analyze the effects of a catheter on the temperature reconstruction process and, as a consequence, its possible application for the

minimization of the effects of strain. Once the plastic bag with warm water inside of it was placed on top of the fiber-optic sensors, the data acquisition process started. It was observed how the temperature readings are changed when the water is cooling down. The result of the experiment with a plastic bag with warm water is shown in Figure 4.3.1.

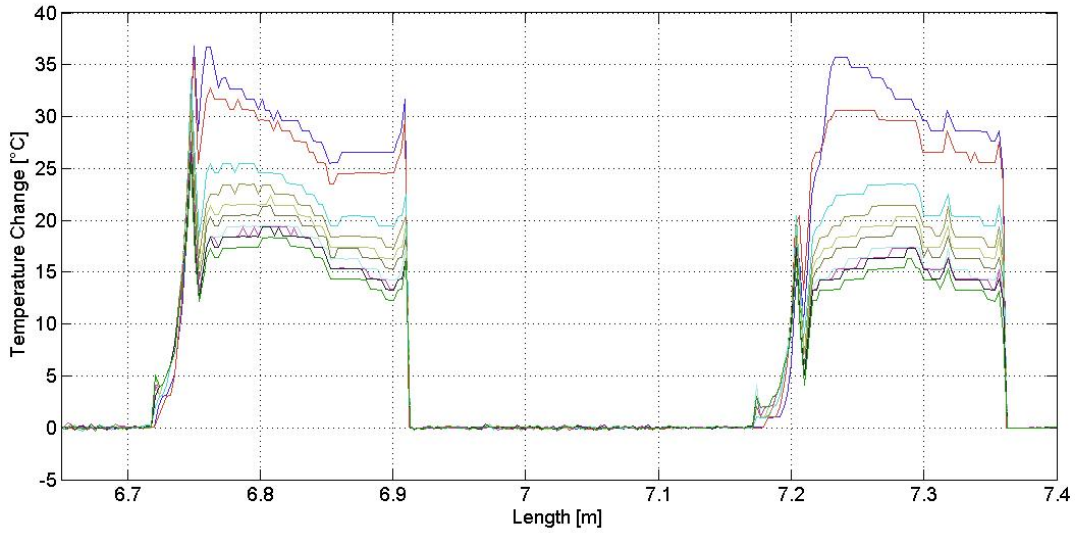

Figure 4.3.1: The representation of the effect of a catheter of the temperature change readings

Considering the room temperature of 21 ˚C, the temperature change was not varied between the 2 sensors after reaching 44 ˚C. Before reaching the temperature of 51 ˚C, the sensor placed inside of a catheter showed the temperature change difference, which was 2.5 ˚C higher in general.

Another experiment was conducted using a beef liver, which was thermally ablated during an RFA experiment. This experiment is considered more suitable for the given application of minimally invasive thermo-therapies. The experimental setup for conducting an RFA experiment with a catheter on a piece of beef liver was shown

in Section 3.3. The results that demonstrate the thermally-ablated tissue are shown in Figures 4.3.2 and 4.3.3.

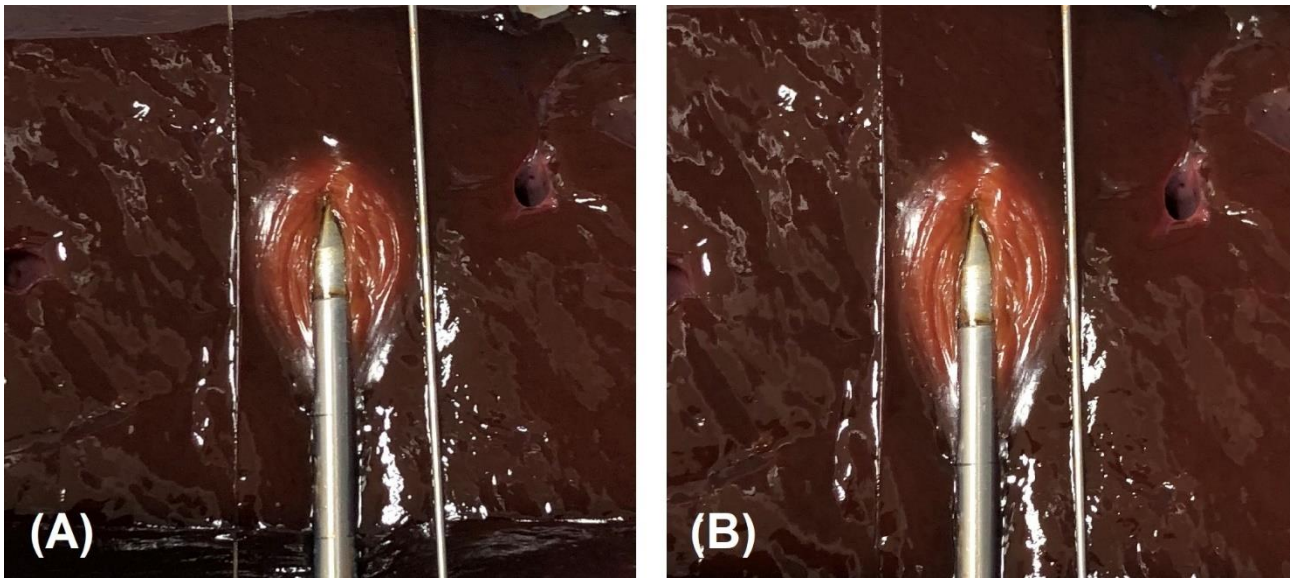

Figure 4.3.2: The initial stages of the RFA process on a piece of a beef liver to analyze the effect of a catheter on the temperature change readings

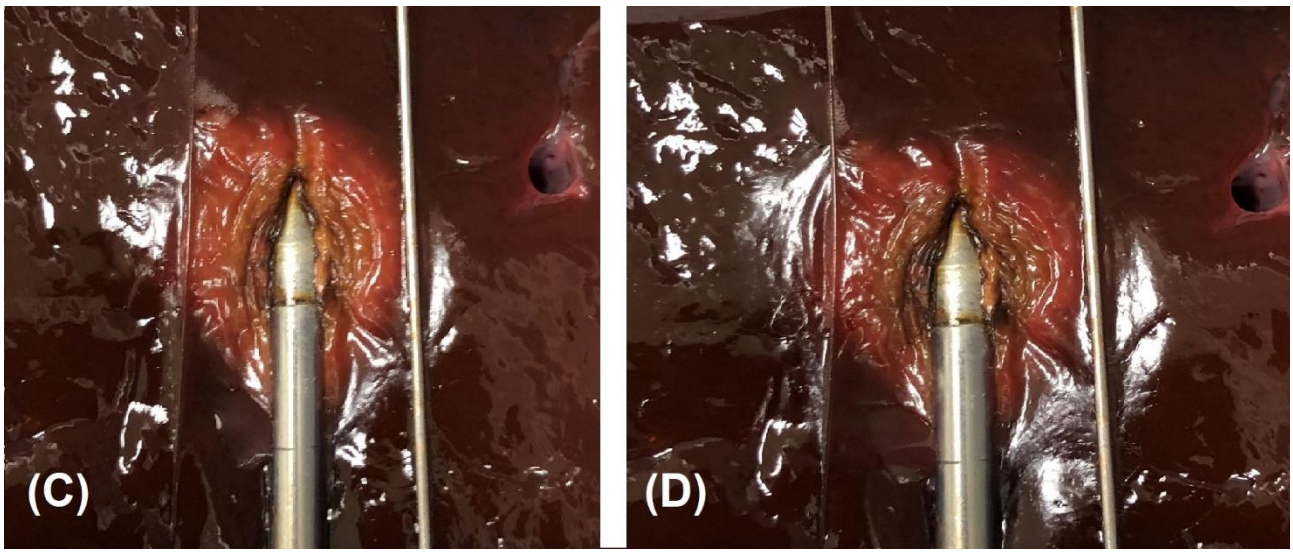

Figure 4.3.3: The final stages of the RFA process on a piece of a beef liver to analyze the effect of a catheter on the temperature change readings

As can be seen the heat propagates through the tissue approximately equally. The results showed that the temperature readings from these 2 sensors were close to each other; however, there were variations in the temperature readings of up to 3 ˚C, Figures 4.3.4 and 4.3.5. This could be explained by not homogeneous type of the tissue and non-ideal placement of the sensors. The maximum temperature achieved by the sensors is identical at the value of 44.5 ˚C, Figure 4.3.5. Overall, the results indicate that the changes in temperature readings of a fiber-optic sensors placed inside of a catheter are not significant and that the catheters can be used in thermal ablation experiments as a solution to avoid the effects of strain.

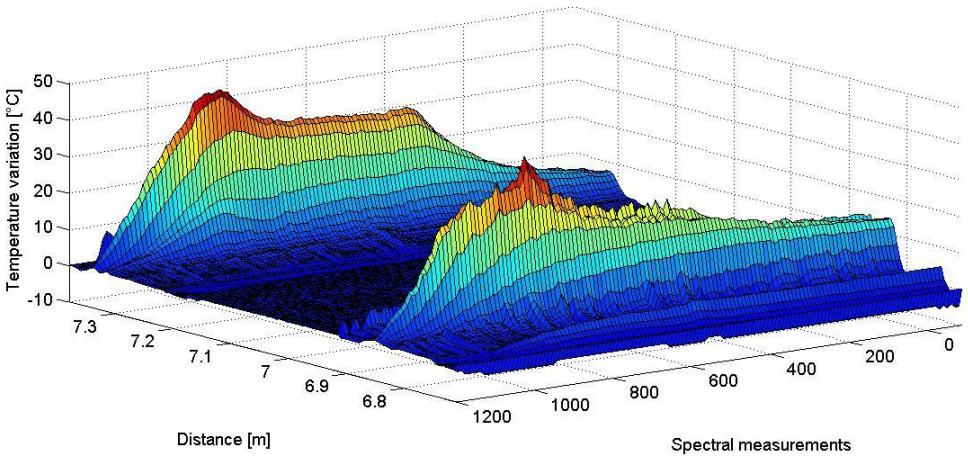

Figure 4.3.4: The effect of a catheter on the temperature change readings of the fiber-optic sensor

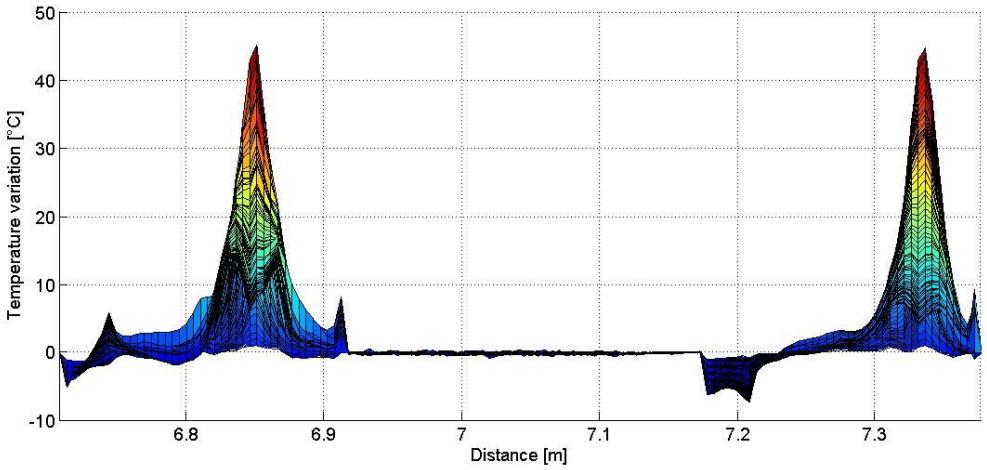

Figure 4.3.5: The effect of a catheter on the temperature change readings of the fiber-optic sensor as a function of distance

Chapter 5 – Conclusion

To summarize, a comparison of various fiber-optic sensing technologies, based on the 5-element FBG array, the CFBG, and the OBR, operating in real-time and suggested to be used for the temperature change monitoring in minimally invasive thermo-therapies for cancer care was provided in this work. The sensors were compared, considering the following criteria: spatial resolution, temperature sensing range, hardware setup, time required for temperature change reconstruction and cost. Also, a HIFU ablation experiment with the 5-element FBG array was conducted in clinical settings to show that the 5-element FBG array can be used as a temperature change monitoring sensor in conjunction with the HIFU equipment for tumor removal in minimally invasive thermo-therapies. Finally, considering the application of the fiber-optic sensors in clinical settings, it was proposed to use a catheter to minimize the effects of strain during the minimally invasive thermo-therapies. The necessary theoretical background was presented in Chapter 2. The conducted work was described in Chapter 3, and the results were presented and discussed in Chapter 4. This chapter allows provided the recommendations for conducting future experiments. The data was gathered by conducting the necessary RFA, HIFU ablation and other experiments. A specific application of these sensors was proposed and described as well. It was suggested to use these fiber-optic sensors in minimally invasive thermo-therapies for cancer care. Overall, considering the minimal invasiveness, low-cost and operation in real-time, these sensors could be applied in the chosen application, with the CFBG

sensor being the most advantageous one compared to its alternatives, which are the 5-element FBG array and the OBR-based sensors.

Bibliography/References

[1] Schena, Emiliano, Daniele Tosi, Paola Saccomandi, Elfed Lewis, and Taesung Kim. "Fiber optic sensors for temperature monitoring during thermal treatments: an overview." *Sensors* 16, no. 7 (2016): 1144.

[2] Korganbayev, Sanzhar, Yerzhan Orazayev, Sultan Sovetov, Ali Bazyl, Emiliano Schena, Carlo Massaroni, Riccardo Gassino et al. "Detection of thermal gradients through fiber-optic Chirped Fiber Bragg Grating (CFBG): Medical thermal ablation scenario." *Optical Fiber Technology* 41 (2018): 48-55.

[3] Mohammed, Anees, and Siniša Djurović. "A study of distributed embedded thermal monitoring in electric coils based on FBG sensor multiplexing." *Microprocessors and Microsystems* 62 (2018): 102-109.

[4] Erdogan, Turan. "Fiber grating spectra." *Journal of lightwave technology* 15, no. 8 (1997): 1277-1294.

[5] Weiss, Noam, S. Nahum Goldberg, Jacob Sosna, and Haim Azhari. "Temperature–density hysteresis in X-ray CT during HIFU thermal ablation: Heating and cooling phantom study." *International Journal of Hyperthermia* 30, no. 1 (2014): 27-35.

[6] Gifford, Dawn K., Brian J. Soller, Matthew S. Wolfe, and Mark E. Froggatt. "Distributed fiber-optic temperature sensing using Rayleigh backscatter." In *Optical Communication, 2005. ECOC 2005. 31st European Conference on*, vol. 3, pp. 511-512. IET, 2005.

[7] Optical Backscatter Reflectometer, Data Sheet, 2018

[8] S. A. Sapareto, “Thermal dose determination in cancer therapy,” Int. J. Radiat. Oncol. Bio. Phys., vol. 10, pp. 787-800, 1984

[9] Goldberg, S. Nahum. "Radiofrequency tumor ablation: principles and techniques." In *Multi-Treatment Modalities of Liver Tumours*, pp. 87-118. Springer, Boston, MA, 2002.

[10] Pereira, Philippe L., Jochen Trübenbach, Martin Schenk, Jörg Subke, Stephan Kroeber, Ines Schaefer, Christopher T. Remy, Diethard Schmidt, Jens Brieger, and Claus D. Claussen. "Radiofrequency ablation: in vivo comparison of four commercially available devices in pig livers." *Radiology* 232, no. 2 (2004): 482-490.

[11] Kennedy, James E. "High-intensity focused ultrasound in the treatment of solid tumours." *Nature reviews cancer* 5, no. 4 (2005): 321.

[12] Dubinsky, Theodore J., Carlos Cuevas, Manjiri K. Dighe, Orpheus Kolokythas, and Joo Ha Hwang. "High-intensity focused ultrasound: current potential and oncologic applications." *American journal of roentgenology* 190, no. 1 (2008): 191-199.

[13] Nikfarjam, Mehrdad, Caterina Malcontenti-Wilson, and Christopher Christophi. "Comparison of 980-and 1064-nm wavelengths for interstitial laser thermotherapy of the liver." *Photomedicine and Laser Therapy* 23, no. 3 (2005): 284-288.

[14] Ierardi, Anna Maria, Alberto Mangano, Chiara Floridi, Gianlorenzo Dionigi, Antonio Biondi, Ejona Duka, Natalie Lucchina, Georgios D. Lianos, and Gianpaolo Carrafiello. "A new system of microwave ablation at 2450 MHz: preliminary experience." *Updates in surgery* 67, no. 1 (2015): 39-45.

[15] Brace, Christopher L. "Radiofrequency and microwave ablation of the liver, lung, kidney, and bone: what are the differences?." *Current problems in diagnostic radiology* 38, no. 3 (2009): 135-143.

[16] Tosi, Daniele, Edoardo Gino Macchi, and Alfredo Cigada. "Fiber-optic temperature and pressure sensors applied to radiofrequency thermal ablation in liver phantom: methodology and experimental measurements." *Journal of Sensors* 2015 (2015).

[17] Exalos Light Source Data Sheet, Retrieved from: http://www.exalos.com/sled-modules/

[18] I-MON High Speed Spectrometer, Retrieved from: https://ibsen.com/products/interrogation-monitors/i-mon-high-speed/
[19] Macchi, Edoardo G., Daniele Tosi, Giovanni Braschi, Mario Gallati, Alfredo Cigada, and Elfed Lewis. "Optical fiber sensors-based temperature distribution measurement in ex vivo radiofrequency ablation with submillimeter resolution." *Journal of biomedical optics* 19, no. 11 (2014): 117004.
[20] Chen, Wei, Riccardo Gassino, Yu Liu, Alessio Carullo, Guido Perrone, Alberto Vallan, and Daniele Tosi. "Performance assessment of FBG temperature sensors for laser ablation of tumors." In *Medical Measurements and Applications (MeMeA), 2015 IEEE International Symposium on*, pp. 324-328. IEEE, 2015.
[21] Korganbayev, Sanzhar, Nurlan Zhakin, Daniele Tosi, Riccardo Gassino, Alberto Vallan, Guido Perrone, Flavia Napoleoni, Emiliano Schena, Paola Saccomandi, and Michele Caponero. "Linearly chirped fiber-optic Bragg grating as distributed temperature sensor for laser ablation." In *SENSORS, 2016 IEEE*, pp. 1-3. IEEE, 2016.
[22] Tosi, Daniele, Sanzhar Korganbayev, Nurlan Zhakin, Riccardo Gassino, Guido Perrone, and Alberto Vallan. "Towards inline spatially resolved temperature sensing in thermal ablation with chirped fiber Bragg grating." In *Medical Measurements and Applications (MeMeA), 2016 IEEE International Symposium on*, pp. 1-6. IEEE, 2016.
[23] Palumbo, Giovanna, Daniele Tosi, Emiliano Schena, Carlo Massaroni, Juliet Ippolito, Paolo Verze, Nicola Carlomagno, Vincenzo Tammaro, Agostino Iadicicco, and Stefania Campopiano. "Real-time temperature monitoring during radiofrequency treatments on ex-vivo animal model by fiber Bragg grating sensors." In *Optical Sensors 2017*, vol. 10231, p. 102312K. International Society for Optics and Photonics, 2017.
[24] Zibaii, Mohammad I., Hamid Latifi, Fatemeh Karami, Abdolaziz Ronaghi, Sara Chavoshi Nejad, and Leila Dargahi. "In vivo brain temperature measurements based on fiber optic Bragg grating." In *Optical Fiber Sensors Conference (OFS), 2017 25th*, pp. 1-4. IEEE, 2017.
[25] Kinet, Damien, Patrice Mégret, Keith Goossen, Liang Qiu, Dirk Heider, and Christophe Caucheteur. "Fiber Bragg grating sensors toward structural health monitoring in composite materials: Challenges and solutions." *Sensors* 14, no. 4 (2014): 7394-7419.
[26] Hill, Kenneth O., and Gerald Meltz. "Fiber Bragg grating technology fundamentals and overview." *Journal of lightwave technology* 15, no. 8 (1997): 1263-1276.
[27] Pisco, Marco, Agostino Iadicicco, Stefania Campopiano, Antonello Cutolo, and Andrea Cusano. "Structured chirped fiber Bragg gratings." *Journal of Lightwave Technology* 26, no. 12 (2008): 1613-1625.
[28] Webb, Heather, Meghan G. Lubner, and J. Louis Hinshaw. "Thermal ablation." In *Seminars in roentgenology*, vol. 46, no. 2, pp. 133-141. WB Saunders, 2011.
[29] SLED Driver Board 5200 Data Sheet, Retrieved from: http://www.exalos.com/sled-driver-boards/
[30] Won, Pei Chin, Jinsong Leng, Yicheng Lai, and John AR Williams. "Distributed temperature sensing using a chirped fibre Bragg grating." *Measurement Science and Technology* 15, no. 8 (2004): 1501.